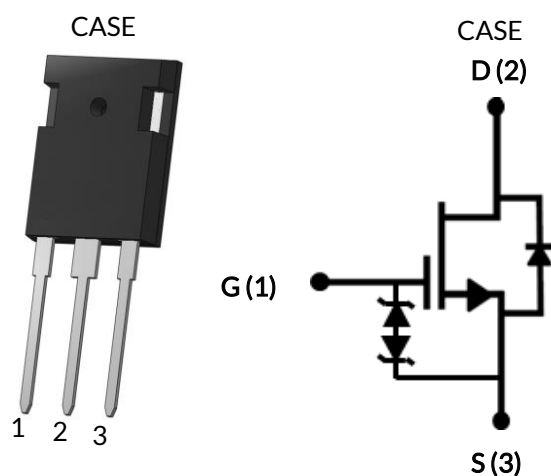


DATASHEET

UJ4C075018K3S



Part Number	Package	Marking
UJ4C075018K3S	TO-247-3L	UJ4C075018K3S



750V-18mΩ SiC FET

Rev. A, October 2020

Description

The UJ4C075018K3S is a 750V, 18mΩ G4 SiC FET. It is based on a unique ‘cascode’ circuit configuration, in which a normally-on SiC JFET is co-packaged with a Si MOSFET to produce a normally-off SiC FET device. The device’s standard gate-drive characteristics allows for a true “drop-in replacement” to Si IGBTs, Si FETs, SiC MOSFETs or Si superjunction devices. Available in the TO-247-3L package, this device exhibits ultra-low gate charge and exceptional reverse recovery characteristics, making it ideal for switching inductive loads and any application requiring standard gate drive.

Features

- ♦ On-resistance $R_{DS(on)}$: 18mΩ (typ)
- ♦ Operating temperature: 175°C (max)
- ♦ Excellent reverse recovery: Q_{rr} = 102nC
- ♦ Low body diode V_{FSD} : 1.14V
- ♦ Low gate charge: Q_G = 37.8nC
- ♦ Threshold voltage $V_{G(th)}$: 4.8V (typ) allowing 0 to 15V drive
- ♦ Low intrinsic capacitance
- ♦ ESD protected, HBM class 2

Typical applications

- ♦ EV charging
- ♦ PV inverters
- ♦ Switch mode power supplies
- ♦ Power factor correction modules
- ♦ Motor drives
- ♦ Induction heating

Maximum Ratings

Parameter	Symbol	Test Conditions	Value	Units
Drain-source voltage	V_{DS}		750	V
Gate-source voltage	V_{GS}	DC	-20 to +20	V
Continuous drain current ¹	I_D	$T_C = 25^{\circ}\text{C}$	81	A
		$T_C = 100^{\circ}\text{C}$	60	A
Pulsed drain current ²	I_{DM}	$T_C = 25^{\circ}\text{C}$	205	A
Single pulsed avalanche energy ³	E_{AS}	$L=15\text{mH}, I_{AS}=3.6\text{A}$	97.2	mJ
Power dissipation	P_{tot}	$T_C = 25^{\circ}\text{C}$	385	W
Maximum junction temperature	$T_{J,max}$		175	$^{\circ}\text{C}$
Operating and storage temperature	T_J, T_{STG}		-55 to 175	$^{\circ}\text{C}$
Max. lead temperature for soldering, 1/8" from case for 5 seconds	T_L		250	$^{\circ}\text{C}$

1. Limited by $T_{J,max}$

2. Pulse width t_p limited by $T_{J,max}$

3. Starting $T_J = 25^{\circ}\text{C}$

Thermal Characteristics

Parameter	Symbol	Test Conditions	Value			Units
			Min	Typ	Max	
Thermal resistance, junction-to-case	$R_{\theta JC}$			0.3	0.39	$^{\circ}\text{C/W}$

Electrical Characteristics ($T_J = +25^\circ\text{C}$ unless otherwise specified)

Typical Performance - Static

Parameter	Symbol	Test Conditions	Value			Units
			Min	Typ	Max	
Drain-source breakdown voltage	BV_{DS}	$V_{GS}=0V, I_D=1mA$	750			V
Total drain leakage current	I_{DSS}	$V_{DS}=750V, V_{GS}=0V, T_J=25^\circ\text{C}$		1.3	125	μA
		$V_{DS}=750V, V_{GS}=0V, T_J=175^\circ\text{C}$		20		
Total gate leakage current	I_{GSS}	$V_{DS}=0V, T_J=25^\circ\text{C}, V_{GS}=-20V / +20V$		4.7	± 20	μA
Drain-source on-resistance	$R_{DS(on)}$	$V_{GS}=12V, I_D=20A, T_J=25^\circ\text{C}$		18	23	m Ω
		$V_{GS}=12V, I_D=20A, T_J=125^\circ\text{C}$		31		
		$V_{GS}=12V, I_D=20A, T_J=175^\circ\text{C}$		41		
Gate threshold voltage	$V_{G(th)}$	$V_{DS}=5V, I_D=10mA$	4	4.8	6	V
Gate resistance	R_G	f=1MHz, open drain		4.5		Ω

Typical Performance - Reverse Diode

Parameter	Symbol	Test Conditions	Value			Units
			Min	Typ	Max	
Diode continuous forward current ¹	I_S	$T_C=25^\circ\text{C}$			81	A
Diode pulse current ²	$I_{S,pulse}$	$T_C=25^\circ\text{C}$			205	A
Forward voltage	V_{FSD}	$V_{GS}=0V, I_F=20A, T_J=25^\circ\text{C}$		1.14	1.46	V
		$V_{GS}=0V, I_F=20A, T_J=175^\circ\text{C}$		1.35		
Reverse recovery charge	Q_{rr}	$V_{DS}=400V, I_S=50A, V_{GS}=-0V, R_{G,EXT}=50\Omega$		102		nC
Reverse recovery time	t_{rr}	di/dt=1300A/ μs , $T_J=25^\circ\text{C}$		25		ns
Reverse recovery charge	Q_{rr}	$V_{DS}=400V, I_S=50A, V_{GS}=-0V, R_{G,EXT}=50\Omega$		109		nC
Reverse recovery time	t_{rr}	di/dt=1300A/ μs , $T_J=150^\circ\text{C}$		27		ns

Typical Performance - Dynamic

Parameter	Symbol	Test Conditions	Value			Units
			Min	Typ	Max	
Input capacitance	C_{iss}	$V_{DS}=100V, V_{GS}=0V$ $f=100kHz$		1422		pF
Output capacitance	C_{oss}			217		
Reverse transfer capacitance	C_{rss}			2		
Effective output capacitance, energy related	$C_{oss(er)}$	$V_{DS}=0V$ to $400V$, $V_{GS}=0V$		150		pF
Effective output capacitance, time related	$C_{oss(tr)}$	$V_{DS}=0V$ to $400V$, $V_{GS}=0V$		280		pF
C_{OSS} stored energy	E_{oss}	$V_{DS}=400V, V_{GS}=0V$		12		μJ
Total gate charge	Q_G	$V_{DS}=400V, I_D=50A$, $V_{GS}=0V$ to $15V$		37.8		nC
Gate-drain charge	Q_{GD}			8		
Gate-source charge	Q_{GS}			11.8		
Turn-on delay time	$t_{d(on)}$	Note 4, $V_{DS}=400V, I_D=50A$, Gate Driver = $0V$ to $+15V$, Turn-on $R_{G,EXT}=1\Omega$, Turn-off $R_{G,EXT}=50\Omega$ Inductive Load, FWD: same device with $V_{GS}=0V, R_G=50\Omega, T_J=25^\circ C$		13		ns
Rise time	t_r			56		
Turn-off delay time	$t_{d(off)}$			139		
Fall time	t_f			21		
Turn-on energy	E_{ON}	FWD: same device with $V_{GS}=0V, R_G=50\Omega, T_J=25^\circ C$		615		μJ
Turn-off energy	E_{OFF}			518		
Total switching energy	E_{TOTAL}			1133		
Turn-on delay time	$t_{d(on)}$	Note 4, $V_{DS}=400V, I_D=50A$, Gate Driver = $0V$ to $+15V$, Turn-on $R_{G,EXT}=1\Omega$, Turn-off $R_{G,EXT}=50\Omega$ Inductive Load, FWD: same device with $V_{GS}=0V, R_G=50\Omega, T_J=150^\circ C$		13		ns
Rise time	t_r			62		
Turn-off delay time	$t_{d(off)}$			147		
Fall time	t_f			22		
Turn-on energy	E_{ON}	FWD: same device with $V_{GS}=0V, R_G=50\Omega, T_J=150^\circ C$		670		μJ
Turn-off energy	E_{OFF}			573		
Total switching energy	E_{TOTAL}			1243		

4. Measured with the half-bridge mode switching test circuit in Figure 28.

Typical Performance - Dynamic (continued)

Parameter	Symbol	Test Conditions	Value			Units
			Min	Typ	Max	
Turn-on delay time	$t_{d(on)}$	Note 5, $V_{DS}=400V$, $I_D=50A$, Gate Driver = 0V to +15V, $R_{G,EXT}=1\Omega$, inductive Load, FWD: same device with $V_{GS}=0V$ and $R_G=1\Omega$, RC snubber: $R_{S1}=10\Omega$ and $C_{S1}=300pF$, $T_J=25^\circ C$		13		ns
Rise time	t_r			61		
Turn-off delay time	$t_{d(off)}$			33		
Fall time	t_f			17		
Turn-on energy including R_S energy	E_{ON}			696		μJ
Turn-off energy including R_S energy	E_{OFF}			217		
Total switching energy	E_{TOTAL}			913		
Snubber R_S energy during turn-on	E_{RS_ON}			4		
Snubber R_S energy during turn-off	E_{RS_OFF}			8		
Turn-on delay time	$t_{d(on)}$	Note 5, $V_{DS}=400V$, $I_D=50A$, Gate Driver = 0V to +15V, $R_{G,EXT}=1\Omega$, inductive Load, FWD: same device with $V_{GS}=0V$ and $R_G=1\Omega$, RC snubber: $R_{S1}=10\Omega$ and $C_{S1}=300pF$, $T_J=150^\circ C$		15		ns
Rise time	t_r			64		
Turn-off delay time	$t_{d(off)}$			36		
Fall time	t_f			18		
Turn-on energy including R_S energy	E_{ON}			744		μJ
Turn-off energy including R_S energy	E_{OFF}			229		
Total switching energy	E_{TOTAL}			973		
Snubber R_S energy during turn-on	E_{RS_ON}			4		
Snubber R_S energy during turn-off	E_{RS_OFF}			8		
Turn-on delay time	$t_{d(on)}$	Note 6, $V_{DS}=400V$, $I_D=50A$, Gate Driver = 0V to +15V, Turn-on $R_{G,EXT}=1\Omega$, Turn-off $R_{G,EXT}=50\Omega$ Inductive Load, FWD: UJ3D06530TS $T_J=25^\circ C$		14		ns
Rise time	t_r			54		
Turn-off delay time	$t_{d(off)}$			139		
Fall time	t_f			21		
Turn-on energy	E_{ON}			619		μJ
Turn-off energy	E_{OFF}			549		
Total switching energy	E_{TOTAL}			1168		
Turn-on delay time	$t_{d(on)}$	Note 6, $V_{DS}=400V$, $I_D=50A$, Gate Driver = 0V to +15V, Turn-on $R_{G,EXT}=1\Omega$, Turn-off $R_{G,EXT}=50\Omega$ Inductive Load, FWD: UJ3D06530TS $T_J=150^\circ C$		14		ns
Rise time	t_r			59		
Turn-off delay time	$t_{d(off)}$			140		
Fall time	t_f			24		
Turn-on energy	E_{ON}			665		μJ
Turn-off energy	E_{OFF}			611		
Total switching energy	E_{TOTAL}			1276		

5. Measured with the chopper mode switching test circuit in Figure 30.

6. Measured with the chopper mode switching test circuit in Figure 29.

Typical Performance Diagrams

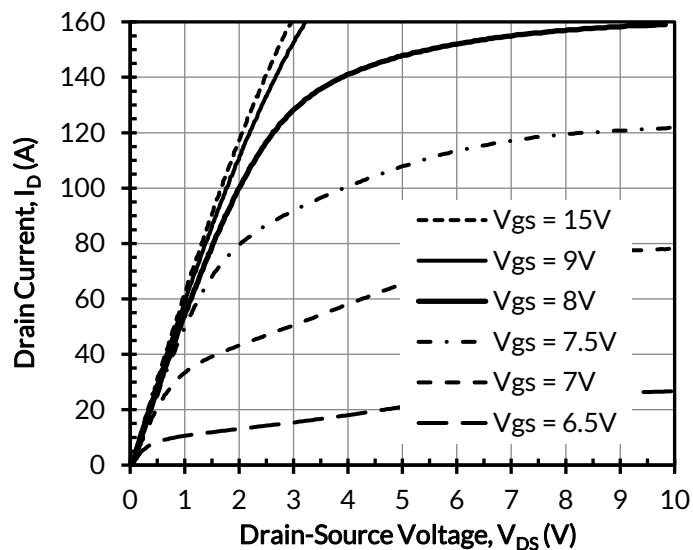


Figure 1. Typical output characteristics at $T_j = -55^\circ\text{C}$, $t_p < 250\mu\text{s}$

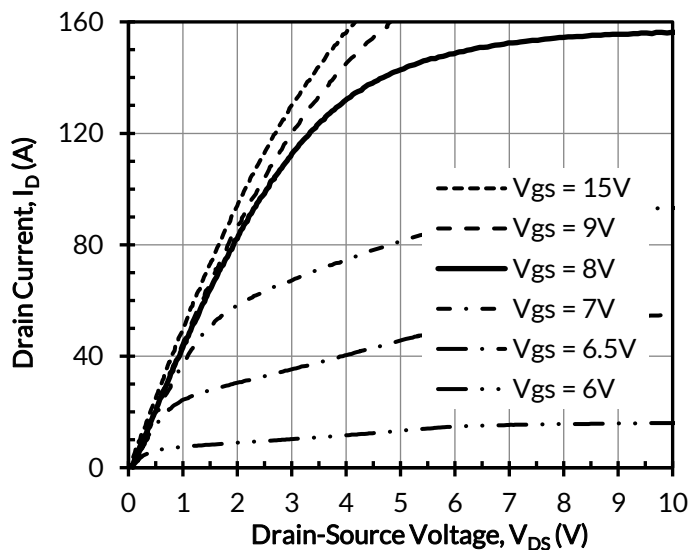


Figure 2. Typical output characteristics at $T_j = 25^\circ\text{C}$, $t_p < 250\mu\text{s}$

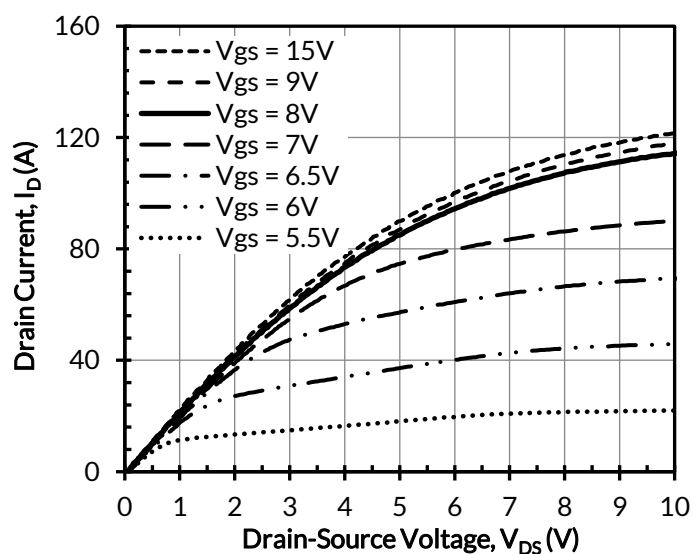


Figure 3. Typical output characteristics at $T_j = 175^\circ\text{C}$, $t_p < 250\mu\text{s}$

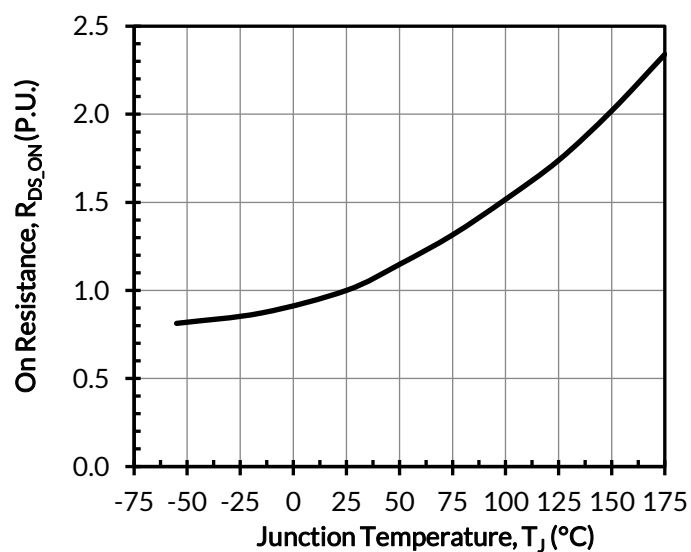


Figure 4. Normalized on-resistance vs. temperature at $V_{GS} = 12\text{V}$ and $I_D = 50\text{A}$

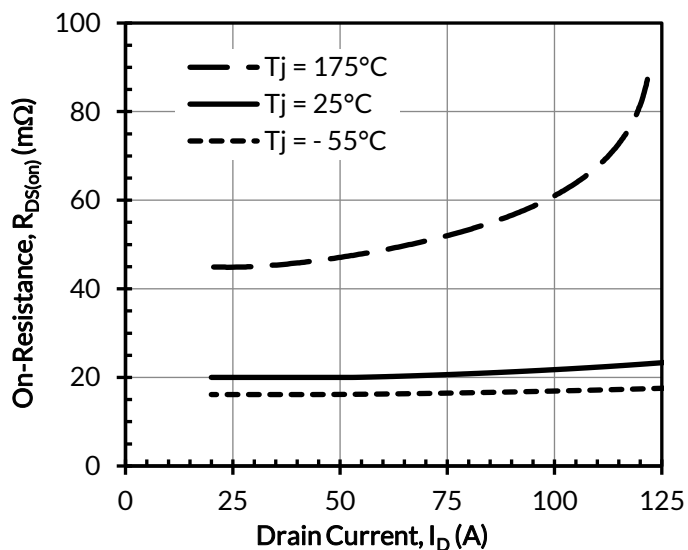


Figure 5. Typical drain-source on-resistances at $V_{GS} = 12V$

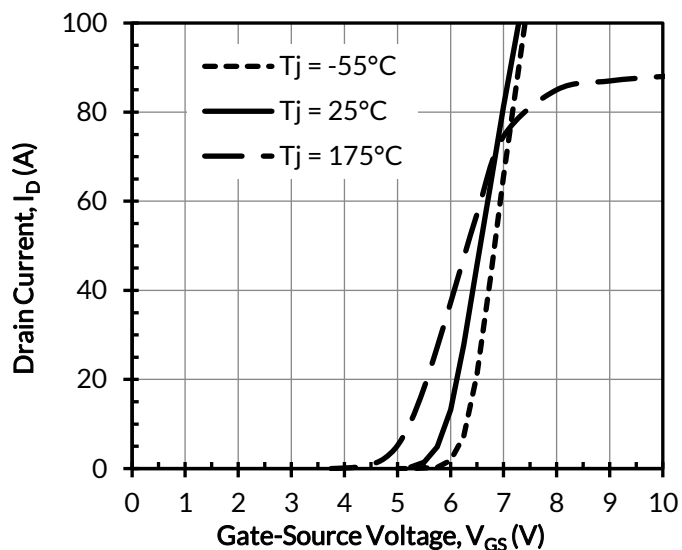


Figure 6. Typical transfer characteristics at $V_{DS} = 5V$

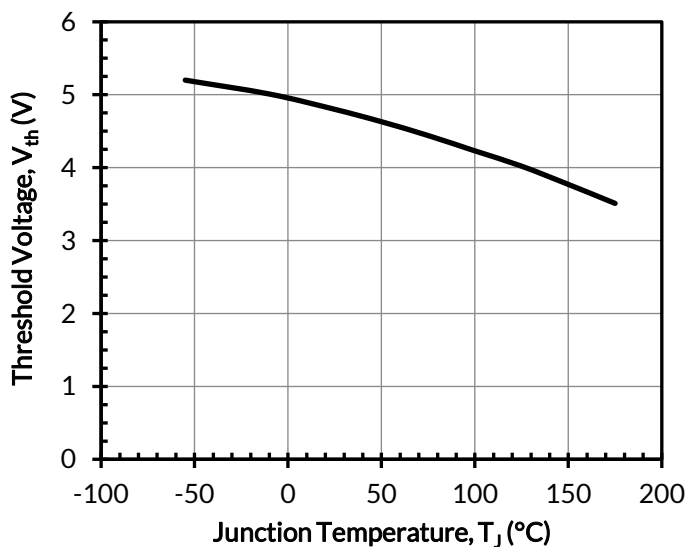


Figure 7. Threshold voltage vs. junction temperature at $V_{DS} = 5V$ and $I_D = 10mA$

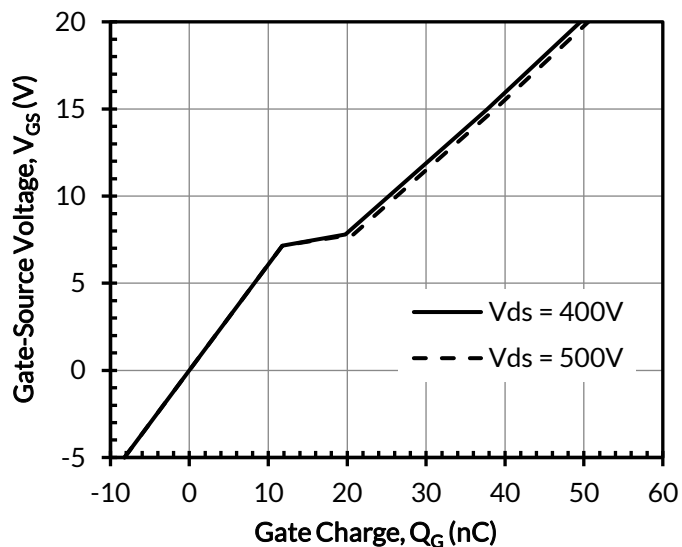


Figure 8. Typical gate charge at $I_D = 50A$

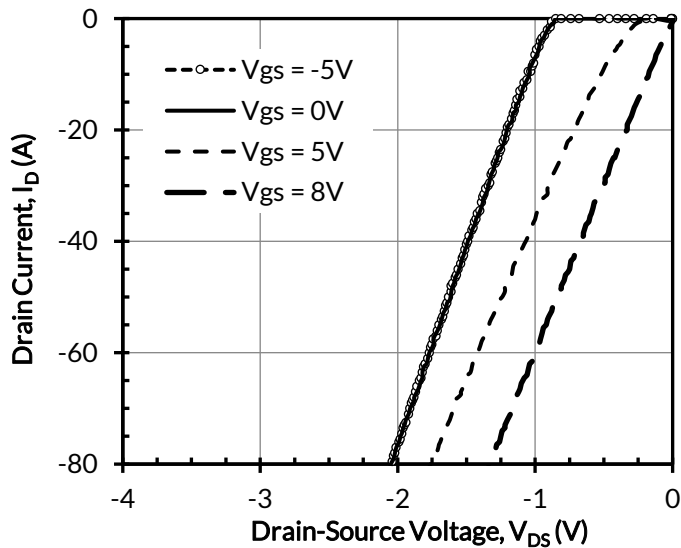


Figure 9. 3rd quadrant characteristics at $T_j = -55^\circ\text{C}$

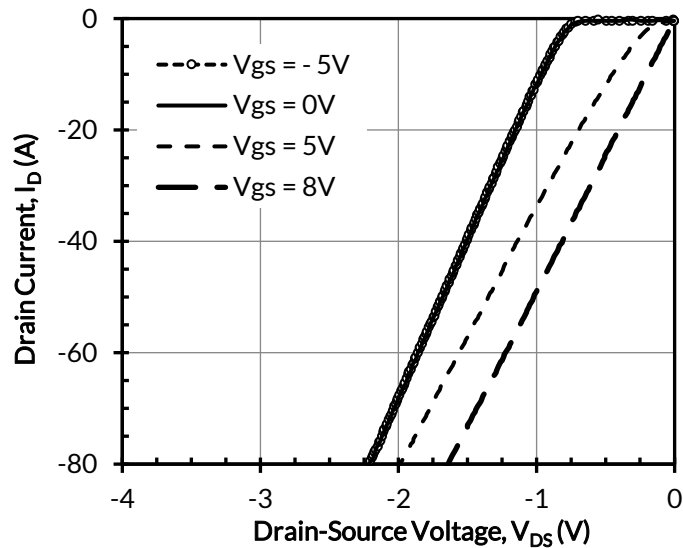


Figure 10. 3rd quadrant characteristics at $T_j = 25^\circ\text{C}$

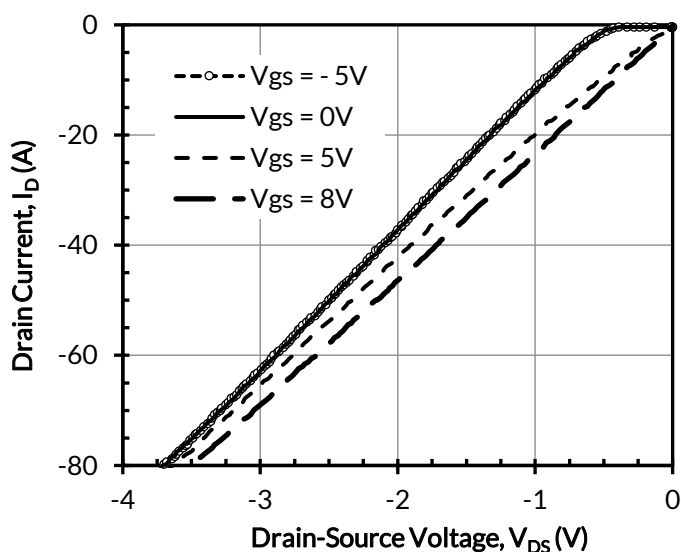


Figure 11. 3rd quadrant characteristics at $T_j = 175^\circ\text{C}$

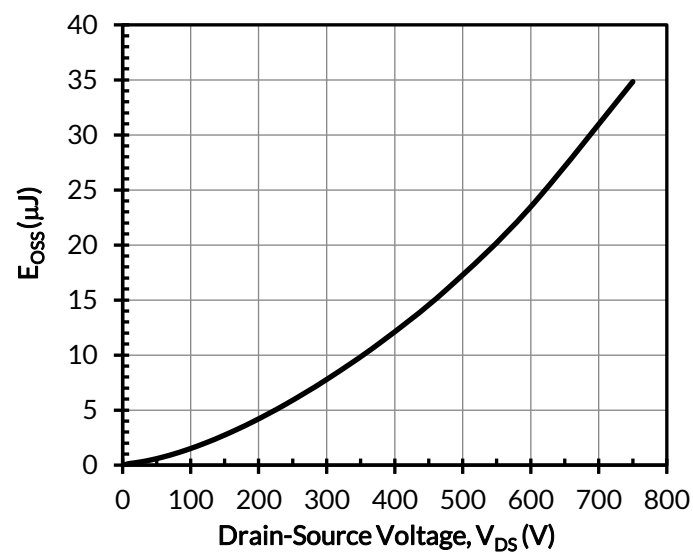


Figure 12. Typical stored energy in C_{oss} at $V_{GS} = 0\text{V}$

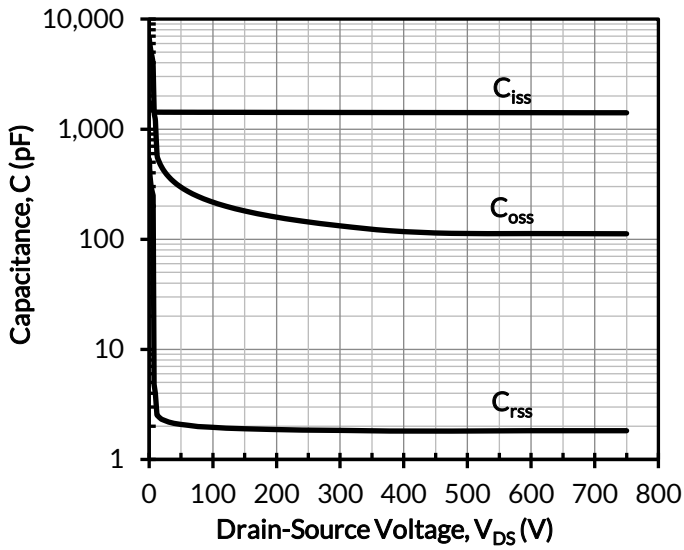


Figure 13. Typical capacitances at $f = 100\text{kHz}$ and $V_{GS} = 0\text{V}$

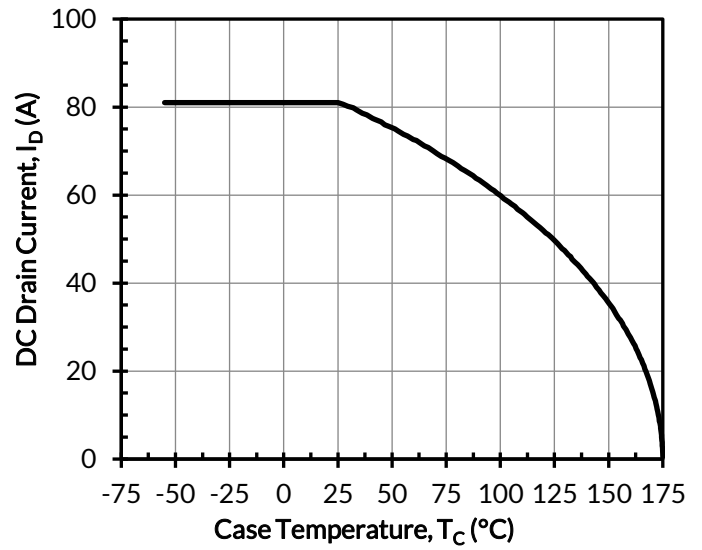


Figure 14. DC drain current derating

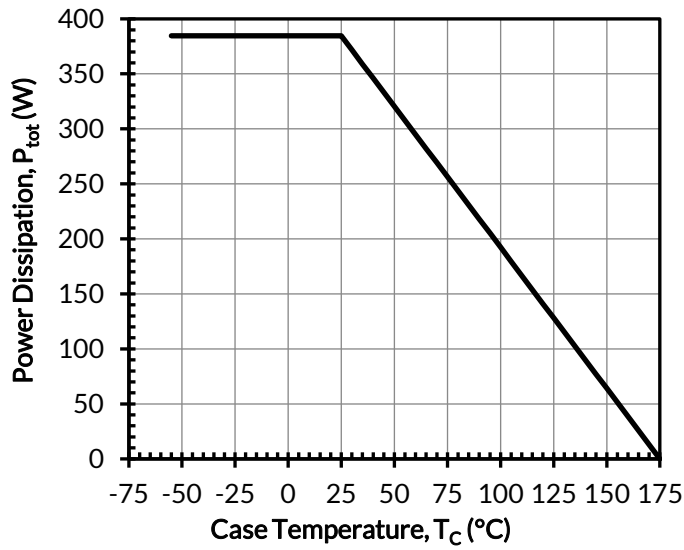


Figure 15. Total power dissipation

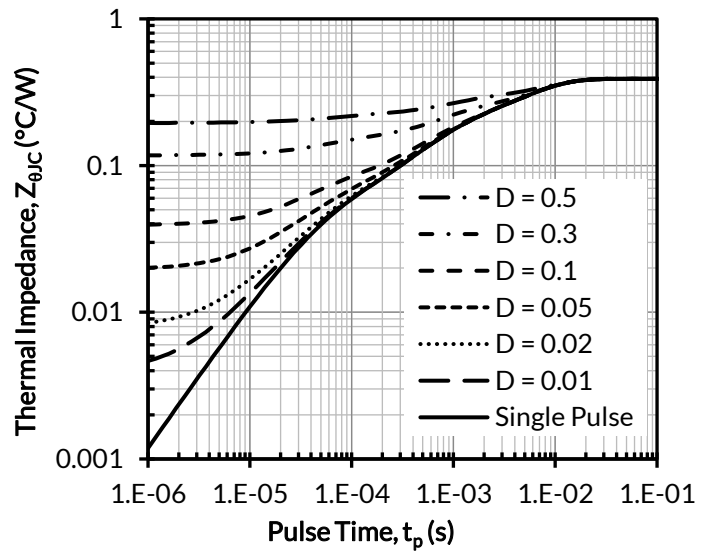


Figure 16. Maximum transient thermal impedance

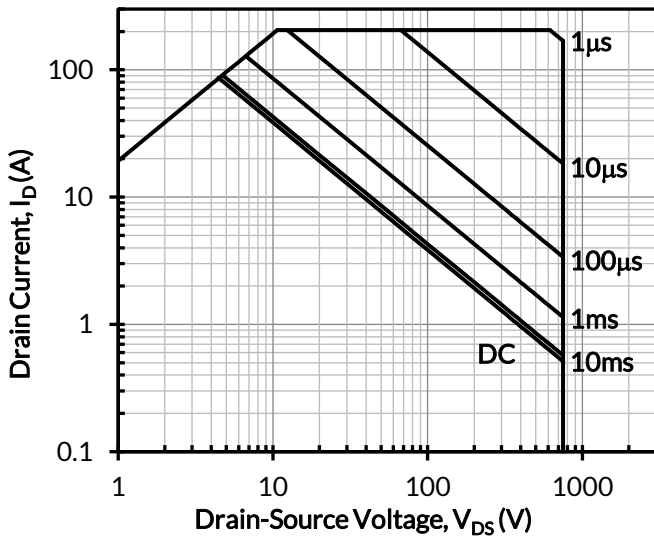


Figure 17. Safe operation area at $T_C = 25^\circ\text{C}$, $D = 0$, Parameter t_p

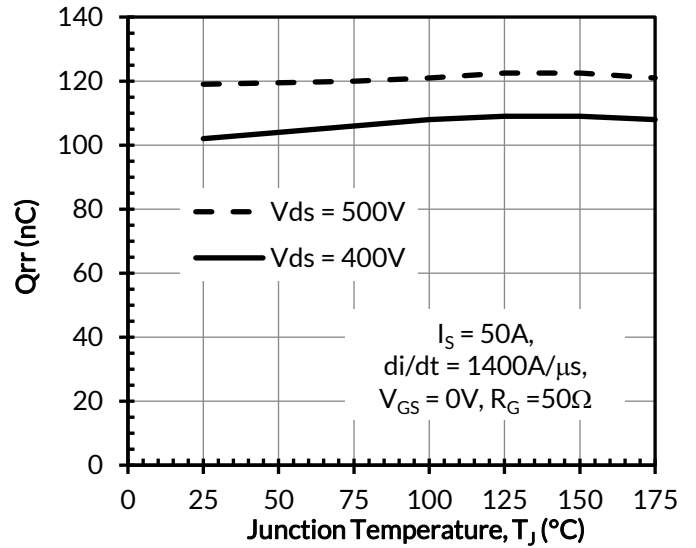


Figure 18. Reverse recovery charge Q_{rr} vs. junction temperature

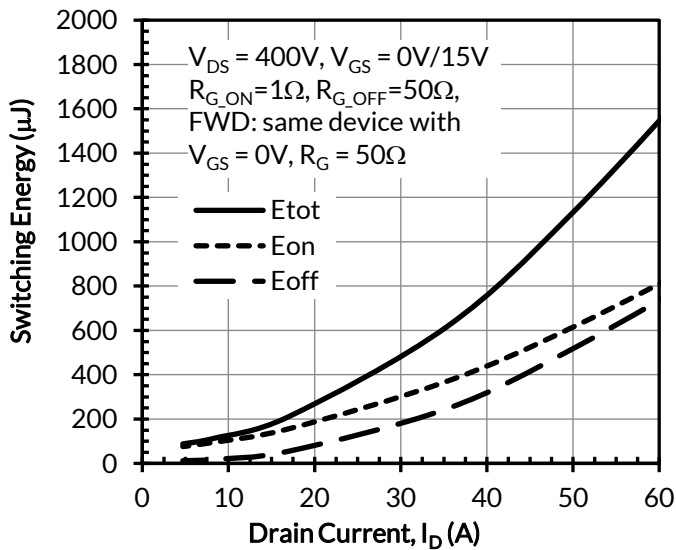


Figure 19. Clamped inductive switching energy vs. drain current at $V_{DS} = 400\text{V}$ and $T_J = 25^\circ\text{C}$

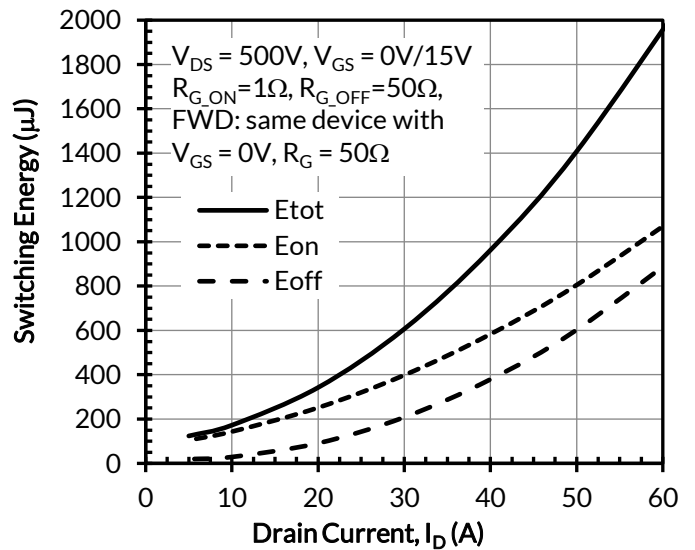


Figure 20. Clamped inductive switching energy vs. drain current at $V_{DS} = 500\text{V}$ and $T_J = 25^\circ\text{C}$

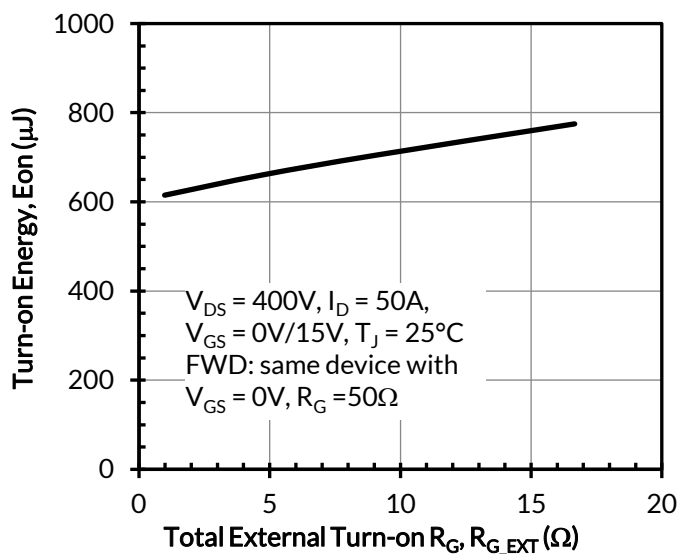


Figure 21. Clamped inductive switching turn-on energy vs. R_{G,EXT_ON}

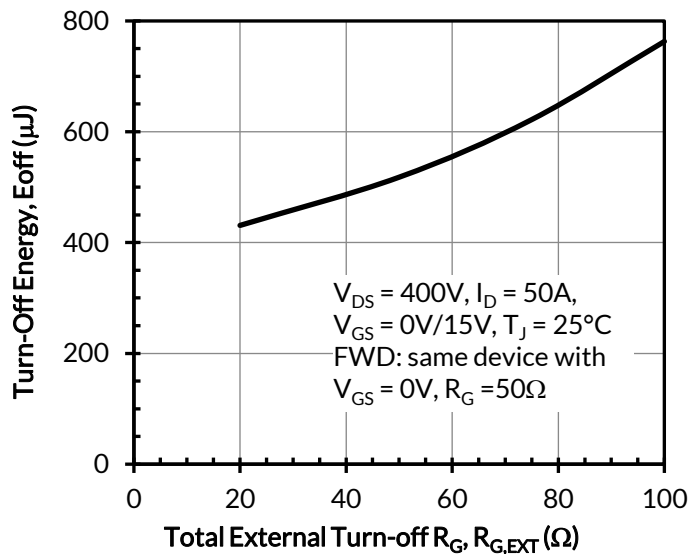


Figure 22. Clamped inductive switching turn-off energy vs. R_{G,EXT_OFF}

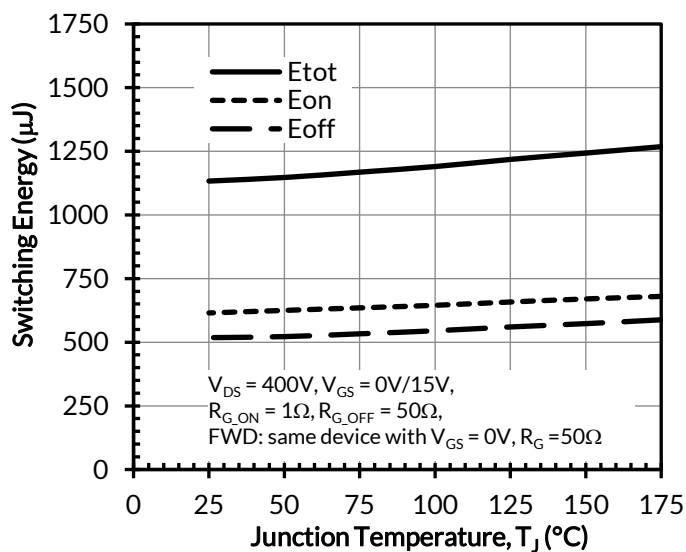


Figure 23. Clamped inductive switching energy vs. junction temperature at $V_{DS} = 400V$ and $I_D = 50A$

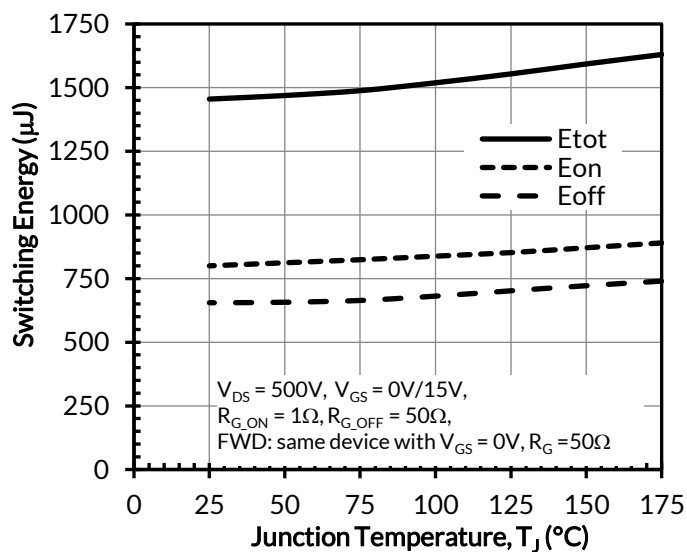


Figure 24. Clamped inductive switching energy vs. junction temperature at $V_{DS} = 500V$ and $I_D = 50A$

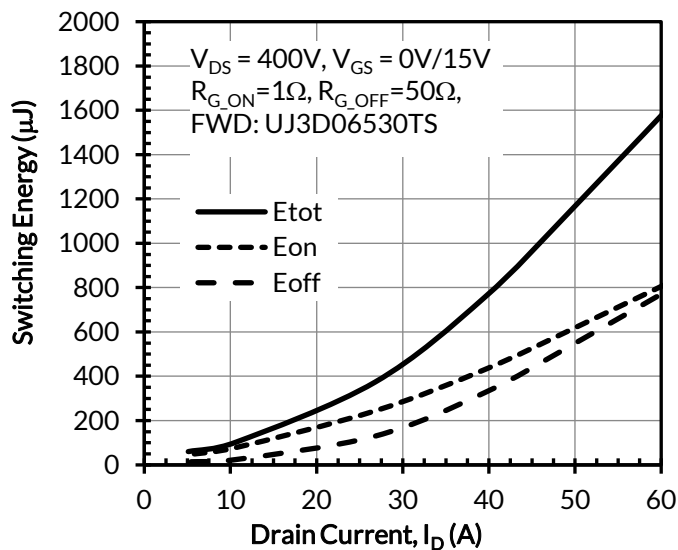


Figure 24. Clamped inductive switching energy vs. drain current at V_{DS} = 400V and T_J = 25°C

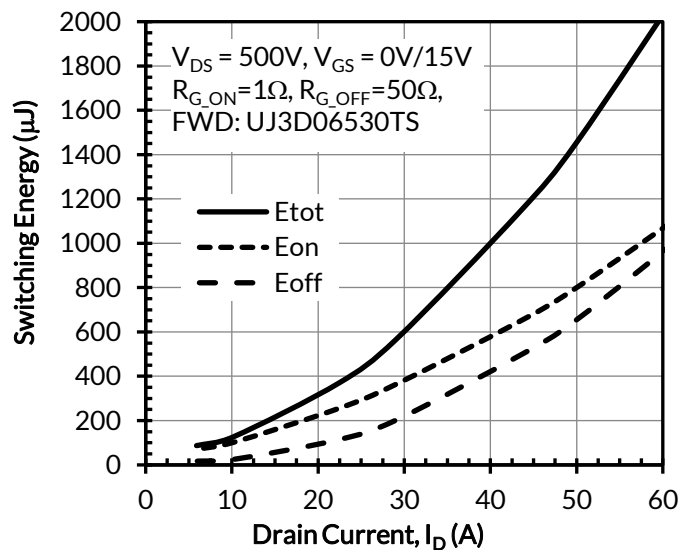


Figure 25. Clamped inductive switching energy vs. drain current at V_{DS} = 500V and T_J = 25°C

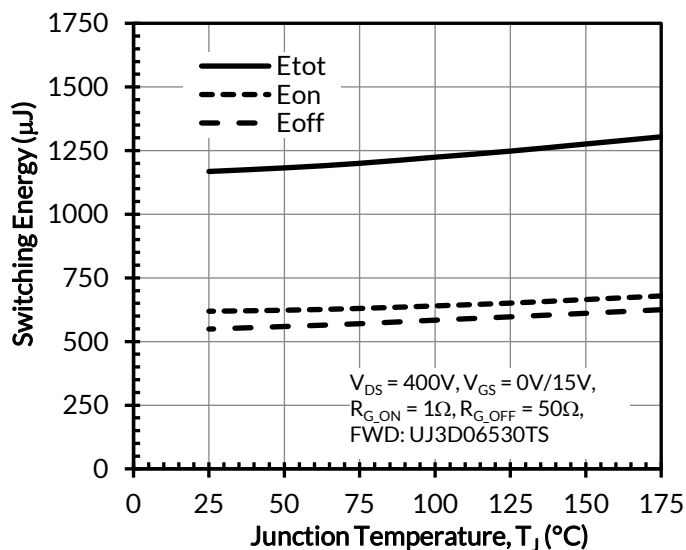


Figure 26. Clamped inductive switching energy vs. junction temperature at V_{DS} = 400V and I_D = 50A

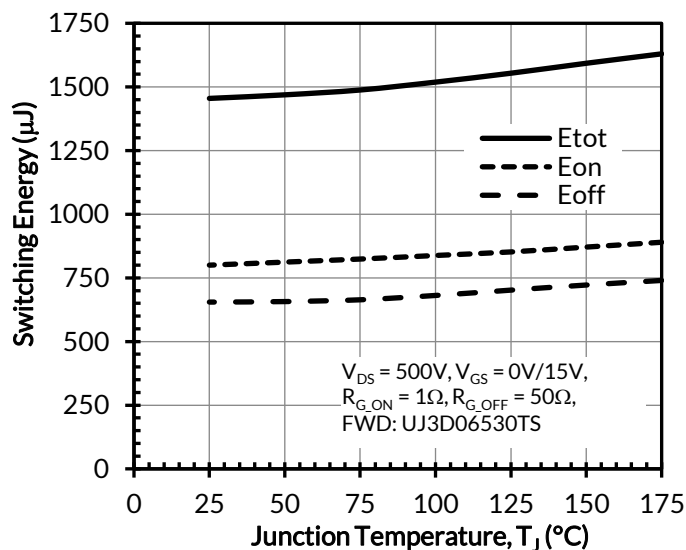


Figure 27. Clamped inductive switching energy vs. junction temperature at V_{DS} = 500V and I_D = 50A

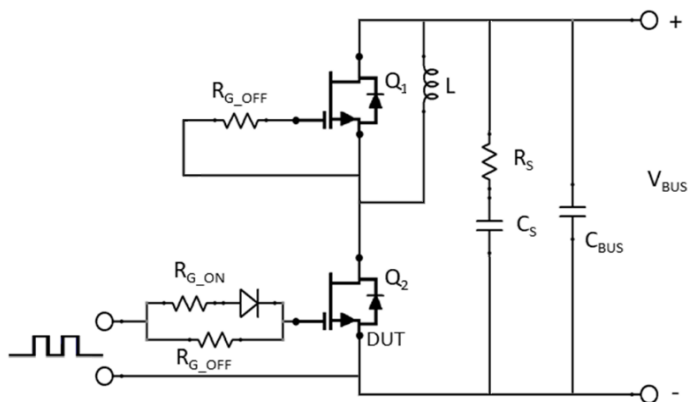


Figure 28. Schematic of the half-bridge mode switching test circuit. Note, a bus RC snubber ($R_S = 2.5\Omega$, $C_S = 100\text{nF}$) is used to reduce the power loop high frequency oscillations.

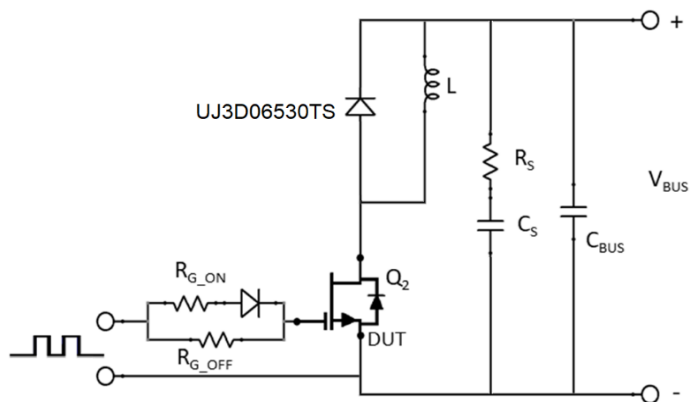


Figure 29. Schematic of the chopper mode switching test circuit. Note, a bus RC snubber ($R_S = 2.5\Omega$, $C_S = 100\text{nF}$) is used to reduce the power loop high frequency oscillations.

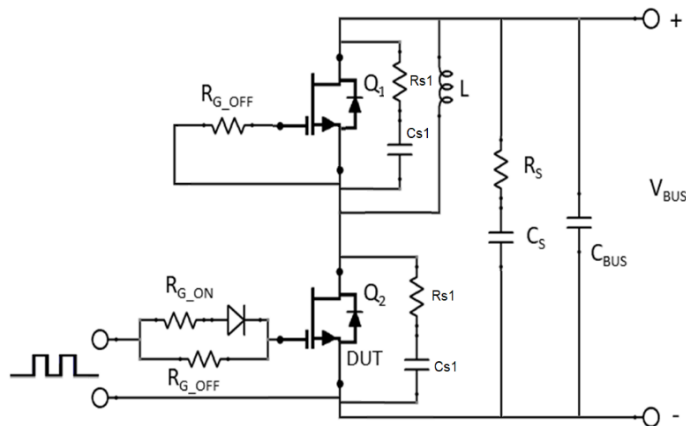


Figure 30. Schematic of the half-bridge mode switching test circuit with device RC snubbers ($R_{S1} = 10\Omega$, $C_{S1} = 300\text{pF}$) and a bus RC snubber ($R_S = 2.5\Omega$, $C_S = 100\text{nF}$).

Applications Information

SiC FETs are enhancement-mode power switches formed by a high-voltage SiC depletion-mode JFET and a low-voltage silicon MOSFET connected in series. The silicon MOSFET serves as the control unit while the SiC JFET provides high voltage blocking in the off state. This combination of devices in a single package provides compatibility with standard gate drivers and offers superior performance in terms of low on-resistance ($R_{DS(on)}$), output capacitance (C_{oss}), gate charge (Q_G), and reverse recovery charge (Q_{rr}) leading to low conduction and switching losses. The SiC FETs also provide excellent reverse conduction capability eliminating the need for an external anti-parallel diode.

Like other high performance power switches, proper PCB layout design to minimize circuit parasitics is strongly recommended due to the high dv/dt and di/dt rates. An external gate resistor is recommended when the FET is working in the diode mode in order to achieve the optimum reverse recovery performance. For more information on SiC FET operation, see www.unitedsic.com.

A snubber circuit with a small $R_{(G)}$, or gate resistor, provides better EMI suppression with higher efficiency compared to using a high $R_{(G)}$ value. There is no extra gate delay time when using the snubber circuitry, and a small $R_{(G)}$ will better control both the turn-off $V_{(DS)}$ peak spike and ringing duration, while a high $R_{(G)}$ will damp the peak spike but result in a longer delay time. In addition, the total switching loss when using a snubber circuit is less than using high $R_{(G)}$, while greatly reducing $E_{(OFF)}$ from mid-to-full load range with only a small increase in $E_{(ON)}$. Efficiency will therefore improve with higher load current. For more information on how a snubber circuit will improve overall system performance, visit the UnitedSiC website at www.unitedsic.com

Disclaimer

UnitedSiC reserves the right to change or modify any of the products and their inherent physical and technical specifications without prior notice. UnitedSiC assumes no responsibility or liability for any errors or inaccuracies within.

Information on all products and contained herein is intended for description only. No license, express or implied, to any intellectual property rights is granted within this document.

UnitedSiC assumes no liability whatsoever relating to the choice, selection or use of the UnitedSiC products and services described herein.

Mouser Electronics

Authorized Distributor

Click to View Pricing, Inventory, Delivery & Lifecycle Information:

Qorvo:

[UJ4C075018K3S](#)